Int. J. Electrochem. Sci., 12 **(2017)** 429 – 439, doi: 10.20964/2017.01.59

International Journal of
ELECTROCHEMICAL
SCIENCE
www.electrochemsci.org

Structure and Electrochemical Properties of $La_4MgNi_{17.5}M_{1.5}$ (M=Co,Fe,Mn) Hydrogen Storage Alloys

Fan-Song Wei[*], *Xin Cai, Yu Zhang, Fan-na Wei*

School of Materials Science and Engineering, Jiangsu University of Science and Technology, Zhenjiang 212003, China
[*]E-mail: zjuwei@just.edu.cn

Received: 11 October 2016 / *Accepted:* 21 November 2016 / *Published:* 12 December 2016

$La_4MgNi_{17.5}M_{1.5}$ (M=Co, Fe, Mn) alloys were prepared by high-frequency inductive melting. The structure and electrochemical properties of the alloy electrodes were systemically investigated. The XRD showed that all the alloys possessed a multiphase structure, consisting of AB_5-type phase and A_5B_{19}-type phase. The result of Rietveld fitting revealed that the cell volume of all the phases was in the order:Co<Fe<Mn. The electrochemical tests indicated that all the alloy electrodes had good activation performance and the maximum discharge capacity of electrodes increases follow the order:Fe<Co<Mn. Meanwhile, the cyclic stability of Fe substitution alloy electrode is worse than that of Co and Mn substitution alloy electrode due to the serious pulverization. Furthermore, it is found that the moderate addition of Co can increase the exchange current density (I_0) of electrodes and the addition of Fe is beneficial for the diffusion of hydrogen atom (D) in the bulk of the electrodes.

Keywords: La-Mg-Ni alloy; hydrogen storage alloy; elements substitution; electrochemical properties

1. INTRODUCTION

As the global energy crisis and environmental pollution become more serious, there are increasing needs for the study of new energy[1-2]. Hydrogen has gotten a lot of attention due to their high energy density and environmental friendliness[3]. As one of the important methods to store hydrogen, hydrogen storage alloys have promoted the development of hydrogen energy[4-5]. Currently, the AB_5-type alloy has been widely used as negative electrode materials in our daily life. However, it can not meet the increasing demand for higher energy density due to its lower discharge capacity (about 320mAh/g) limited by single $CaCu_5$-type structure[6].

In recent years, La-Mg-Ni-system alloys have been extensively studied for their high discharge capacity and good high rate dischargeability (HRD) [7-9]. Kohno[10] et al found that the maximum

discharge capacity of La-Mg-Ni system alloys can reach to 410mAh/g, which is 25% higher than that of AB_5-type alloys. Ouyang[11] et al found that the HRD of $La_{11.3}Mg_{6.0}Sm_{7.4}Ni_{61.0}Co_{7.2}Al_{7.1}$ alloy at 1750mA/g could increase to 89.6%. Ternary La-Mg-Ni alloys are mainly composed of one or some of $PuNi_3$-type ($LaNi_5$+2$LaMgNi_4$), Ce_2Ni_7-type ($LaNi_5$+$LaMgNi_4$) and Pr_5Co_{19}-type (3$LaNi_5$+2$LaMgNi_4$), in which [$LaNi_5$] units and [$LaMgNi_4$] units alternatively stack along c-axis in certain ratios[12]. It is studied that the cell volume expansion rate ($\Delta V/V$) of AB_3-type alloy after hydrogen absorbing is larger[13]. Thus the AB_3-type alloy is easier to be pulverised during cycling, and shows poor cycling stability. Compared with $PuNi_3$-type alloys, Ce_2Ni_7-type (2H) alloys show better cyclic stability[14-15], but it needs to be further improved to meet the practical application. Li[16] et al found that the corrosion rate of various phases are in order: $CeNi_3$>Ce_2Ni_7>$CaCu_5$>Ce_5Co_{19}, and it is revealed that heat treatment and partial substitution are two effective ways to change the cycle life of alloy electrodes. Deng[17] et al found that the suitable annealing temperature is beneficial for the formation of A_5B_{19}-type phase. It is reported that the comprehensive electrochemical properties of hydrogen storage alloys can be improved obviously by partial substituting Co for Ni[18-19]. Meanwhile, Mn addition can not only decrease the equilibrium plateau pressure, but also improve the reversible capacity of alloys[20-21]. Moreover, Fe partial substitution for Ni can lower the expansion rate of cell volume and strengthen the anti-pulverization ability of alloys[22-23]. Thus, the A_5B_{19}-type $La_4MgNi_{17.5}M_{1.5}$ (M=Co, Fe, Mn) hydrogen storage alloys were prepared by vacuum melting and then annealed at 1173K for 8h. And the effects of different element substitution as the B-side component on the phase structure and electrochemical properties were systematically studied.

2. EXPERIMENTAL

The $La_4MgNi_{17.5}M_{1.5}$ (M=Co,Fe,Mn) alloys were prepared by vacuum levitation under argon atmosphere. The alloy samples were mechanically crushed into powders of 300 mesh size for X-ray diffraction (XRD) analysis and electrochemical tests.

XRD measurements were performed on a X-ray diffractometer-600 with Cu Kα radiation. The patterns were recorded over the range from 18° to 75° in 2θ by a step of 3^o/min. The lattice parameters and phase abundance were analyzed by using Rietica software. For electrochemical tests, alloy electrodes were prepared by cold pressing the mixture of alloy powder and carbonyl nickel powder at the weight ratio of 1:4 under 18MPa pressure to form a pellet (Φ10mm×1mm). The pulverization of electrodes were examined by scanning electron microscope (SEM). Electrochemical measurements were performed at 298K in standard open tri-electrode electrolysis cell, consisting of a working electrode, a sintered counter electrode ($Ni(OH)_2$/NiOOH) and a reference electrode (Hg/HgO) immersed in 6mol/L KOH electrolyte.

Each electrode was charged at 120mA/g for 4h and then discharged at 60mA/g after 5 min rest for activation. The cyclic test was performed at the charge/discharge current of 300mA/g and the high-rate dischargeability (HRD) was calculated by measuring the discharge capacity at different discharge

current density. All the tests above were discharged to the same cut-off potential of -0.7V (v.s. Hg/HgO).

In order to further investigate the electrochemical kinetic characteristic of electrodes, the linear polarization was plotted by scanning the electrode potential at the rate of 0.1mV/s from -5mV to 5mV at 50% depth of discharge (DOD), and the hydrogen diffusion coefficient was estimated by the potentiostatic discharge via discharging the electrodes at the constant potential-step of 600mV for 3000s after being fully charged.

3. RESULTS AND DISCUSSION

3.1 Phase structure

Fig.1 shows the XRD patterns of $La_4MgNi_{17.5}M_{1.5}$ (M=Co,Fe,Mn) alloys. It can be seen that all the substituted alloys are composed of $(La,Mg)_5Ni_{19}$ phase (Pr_5Co_{19}+Ce_5Co_{19} structure) and $LaNi_5$ phase ($CaCu_5$ structure).

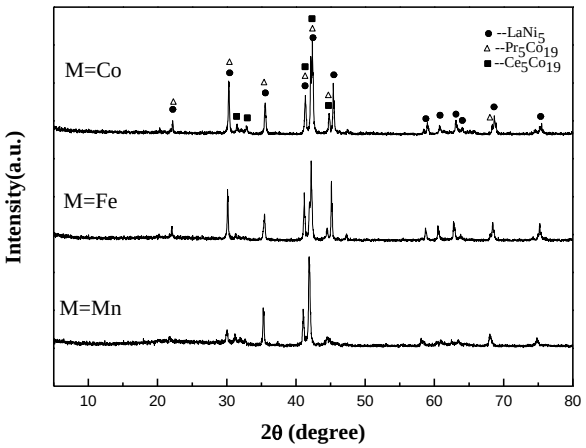

Figure 1. XRD patterns of $La_4MgNi_{17.5}M_{1.5}$ (M=Co,Fe,Mn) alloys

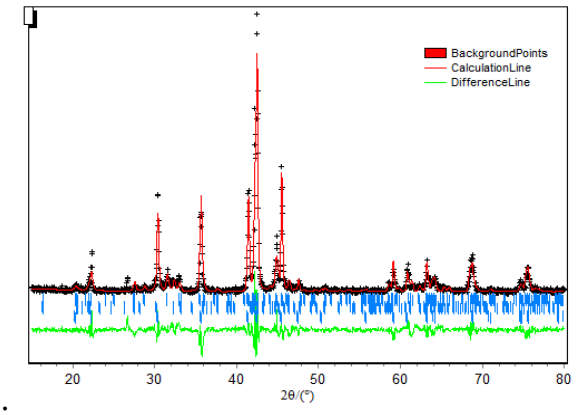

Figure 2. XRD patterns and Rietveld fitting curves of $La_4MgNi_{17.5}Co_{1.5}$ alloy

Fig.2 shows the Rietveld fitting curves of $La_4MgNi_{17.5}Co_{1.5}$ alloy (Rwp= 18.25). The result reveals that Mg atom occupies the 4f and 6c position of La atom in the Laves phase unit of A_5B_{19}-type phase (Pr_5Co_{19} + Ce_5Co_{19} structure), which is same as that of PuNi3-type phase.

The results of Rietveld whole pattern fitting of all the alloys are listed in Table 1. It can be seen that the alloy substituted by Mn possesses the maximum of phase abundance of A_5B_{19}-type phase (74.6%). It is also found that the substitution of Co, Fe and Mn make the cell volume of all the phases increase and the order is: Co<Fe<Mn, which is consistent with the atomic radius of these element[24] (Co=0.125, Fe=0.126, Mn=0.137).

Table 1. The phase structure and lattice parameters of $La_4MgNi_{17.5}M_{1.5}$ (M=Co, Fe, Mn) alloys

Alloy	Type of phase	Space group (No.)	Phase abundance (%)	Lattice constants a/nm	c/nm	V (10^{-3}nm^3)
$La_4MgNi_{17.5}Co_{1.5}$	Pr_5Co_{19}	$P6_3/mmc$(194)	28.5	0.5035	3.2440	714.28
	Ce_5Co_{19}	R-3m(166)	44.1	0.4938	4.8718	1030.73
	$LaNi_5$	P6/mmm(191)	27.4	0.5011	0.3911	85.05
$La_4MgNi_{17.5}Mn_{1.5}$	Pr_5Co_{19}	$P6_3/mmc$(194)	31.7	0.5071	3.2471	718.61
	Ce_5Co_{19}	R-3m(166)	42.9	0.4948	4.8743	1033.28
	$LaNi_5$	P6/mmm(191)	25.4	0.5015	0.3983	86.76
$La_4MgNi_{17.5}Fe_{1.5}$	Pr_5Co_{19}	$P6_3/mmc$(194)	10.1	0.5048	3.2499	717.15
	Ce_5Co_{19}	R-3m(166)	21.5	0.4949	4.8706	1032.94
	$LaNi_5$	P6/mmm(191)	68.4	0.5005	0.3974	86.68

3.2 Activation performance and discharge capacity

Table 2. The electrochemical properties of $La_4MgNi_{17.5}M_{1.5}$ (M=Co, Fe, Mn) alloy electrodes

Samples	N_a	C_{max} (mAh/g)	S_{100} (%)
M=Co	2	358.6	69.3
M=Fe	3	321.0	58.7
M=Mn	2	367.3	68.1

Table 2 lists the electrochemical properties of $La_4MgNi_{17.5}M_{1.5}$ (M=Co, Fe, Mn) alloys. All the alloy electrodes exhibit good activation performance, and can be activated within 3 cycles. From Table 2, it can be seen that the maximum discharge capacities of the alloys show the order: Mn>Co>Fe, and this results maybe relate to the changes of phase abundance and cell volume. As is known, the A_5B_{19}-type phase owns higher hydrogen storage capacity than AB_5-type phase and the larger cell volume is

beneficial for hydrogen atom to enter the alloys[25], so the Mn substituted alloy possesses the highest discharge capacity of 367.3mAh/g.

3.3 Cyclic stability

Fig.3 shows the cyclic stability curves of $La_4MgNi_{17.5}M_{1.5}$(M=Co, Fe, Mn) alloy electrodes. It is observed that the Mn and Co substitution alloys have better capacity retention(S_{100}), which is 68.1% and 69.3%, respectively. The Fe substitution alloy shows worse cyclic stability, which is different from the result reported before[26-28].

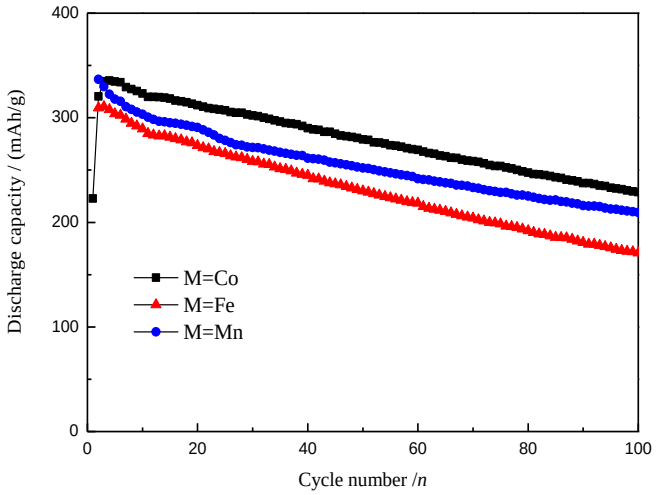

Figure 3. Cyclic stability curves of $La_4MgNi_{17.5}M_{1.5}$ (M=Co, Fe, Mn) alloy electrodes

In order to investigate the causes, the SEM observation on the alloy electrodes after 100 cycles are performed and showed in Fig.4. It can be seen that the alloy bulks in Mn and Co substitution electrodes still keep a whole after 100 cycles, while the Fe substitution electrode has crumbled into small particles.

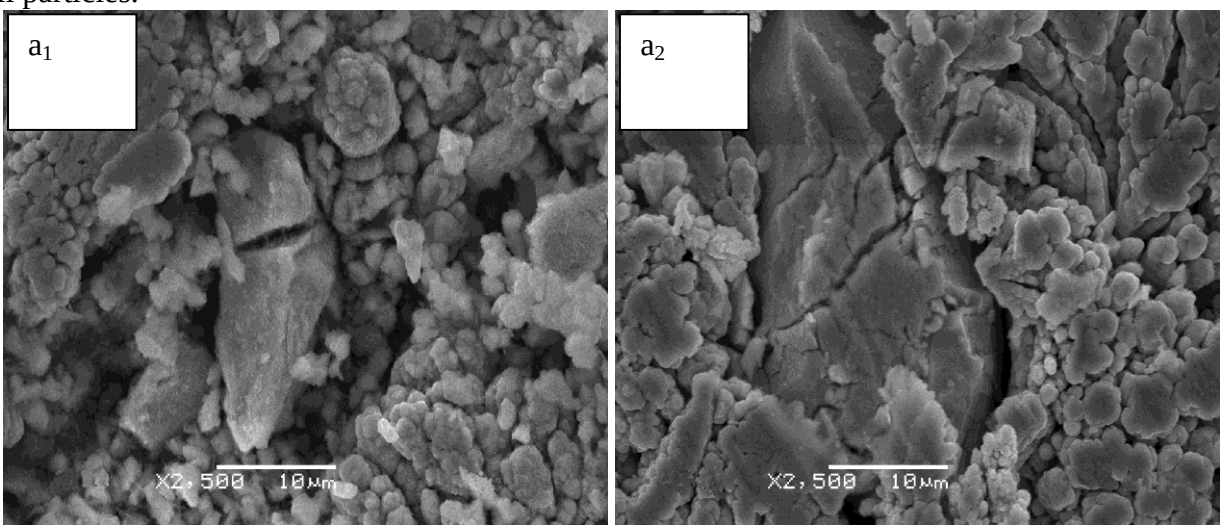

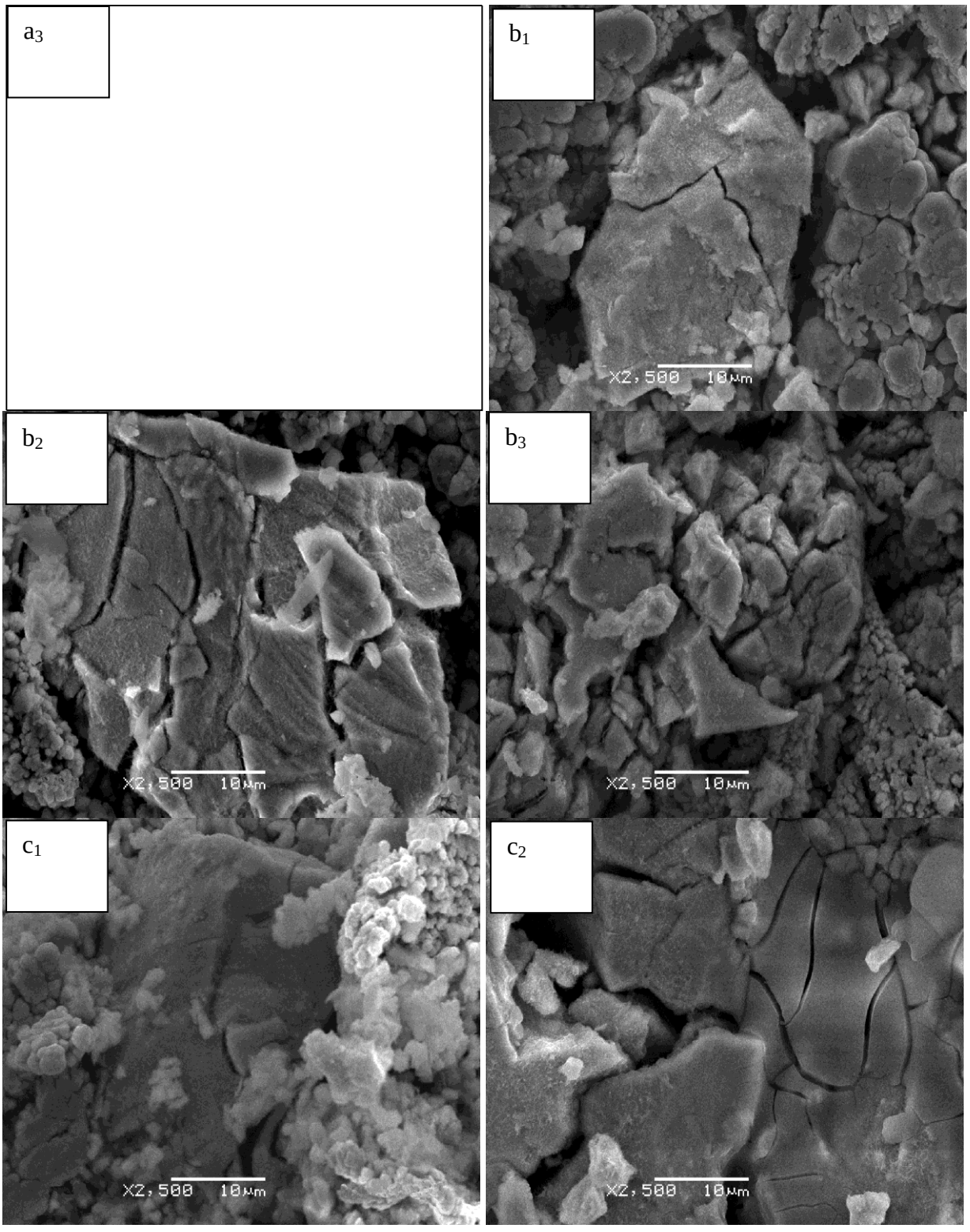
a3
b1
XZ,500 10μm
b2
XZ,500 10μm
b3
XZ,500 10μm
c1
XZ,500 10μm
c2
XZ,500 10μm

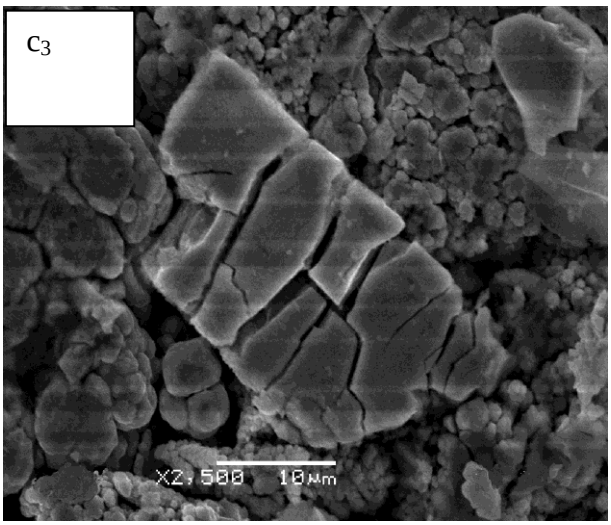

Figure 4. SEM images of the pulverization of $La_4MgNi_{17.5}M_{1.5}$ (M=Co, Fe, Mn) alloy electrodes with different charge/discharge cycles: a_1, b_1, c_1; a_2, b_2, c_2; a_3, b_3, c_3 denote 0, 50, 100 cycles, respectively

It is recognized that the serious pulverization makes more surface exposed to the corrosive electrolyte and corroded. Thus the pulverization degree of alloy electrodes is in accordance with the changes of cycle life.

3.4 P-C-T isotherms

The pressure-concentration-temperature (P-C-T) isotherms of the alloys are shown in Fig.5. There are two obvious plateaus in the Co substitution alloy, while those in the Fe and Mn-substitution alloys are not apparent.

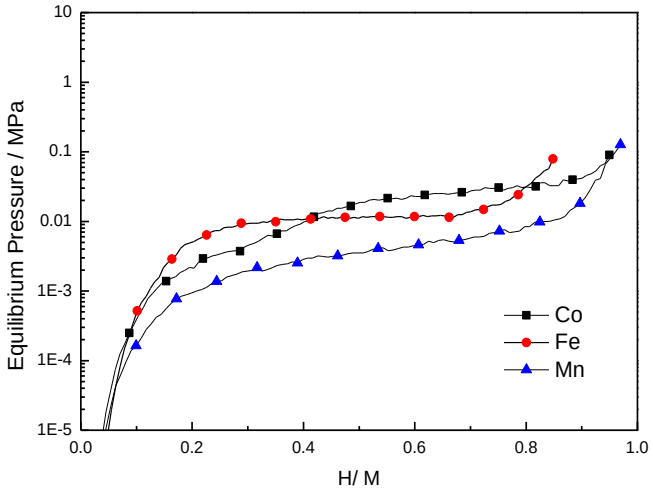

Figure 5. The P-C-T isotherms of $La_4MgNi_{17.5}M_{1.5}$ (M=Co,Fe,Mn) alloy electrodes

The two plateau regions belong to the AB_5-type phase (higher plateau pressure) and A_5B_{19}-type phase (lower plateau pressure), respectively[29]. It also can be found that the plateau pressure of the substituted alloys are in the order: Co>Fe>Mn, which correspond to the study reported by Huang[30] et al that the increase of cell volume could decrease the pressure of hydrogen absorption. The hydrogen storage capacity of alloy electrodes also matches well with the discharge capacity of them.

3.5 High rate dischargeability

High rate dischargeability (HRD) is an important parameter for the batteries and can be defined by the following equation:

$$HRD_d = \frac{C_d}{C_d + C_{60}} \times 100\% \quad (1)$$

where C_d is the discharge capacity at a discharge current density of I_d, and C_{60} is the residual discharge capacity at 60mA/g after the alloy electrode has been fully discharged at I_d. Table 3 lists the HRD and related kinetic properties of electrodes. It can be found that the Fe and Co-substituted alloys possess better HRD at the discharge current of 900mA/g, which is up to 93.58% and 92.81%, respectively.

Table 3. Electrochemical kinetics properties of $La_4MgNi_{17.5}M_{1.5}$ (M=Co, Fe, Mn) alloy electrodes

Samples	HRD (%)			I_0 (mA/g)	D $\times 10^{-10}$ cm^2s^{-1}
	HRD_{300}	HRD_{600}	HRD_{900}		
M=Co	98.60	95.57	92.81	240.23	1.108
M=Fe	98.05	95.43	93.58	208.41	1.581
M=Mn	96.31	88.35	79.26	221.45	0.971

In general, the HRD of electrode is mainly controlled by the charge exchange rate on the surface of alloy and the diffusion rate of hydrogen atom in the crystal lattice[31]. In order to further study the dynamics performance of the alloy electrodes, the linear polarization curves and the constant potential step curves are performed to calculate the the exchange current density (I_0) and the hydrogen diffusion coefficient (D), respectively.

I_0 is calculated by the equation[32]:

$$I_0 = \frac{RT}{FR_p} \quad (2)$$

where R is the molar gas constant, T is the ambient temperature (298K) and F is the Faraday constant.

D is calculated by the equation[33]:

$$\lg i = \lg(\frac{6FD}{da^2}(C_0 - C_s)) - \frac{\pi^2}{2.303}\frac{D}{a^2}t \quad (3)$$

where a is the particle radius, i is the diffusion current density, C_0 is the initial hydrogen concentration inside the alloy, C_s is the hydrogen concentration on the granule surface, d is the hydrogen storage alloy's density and t is the discharge time. The linear polarization curves and the log(i)-time responses curves are presented in Fig.6 and Fig.7, respectively.

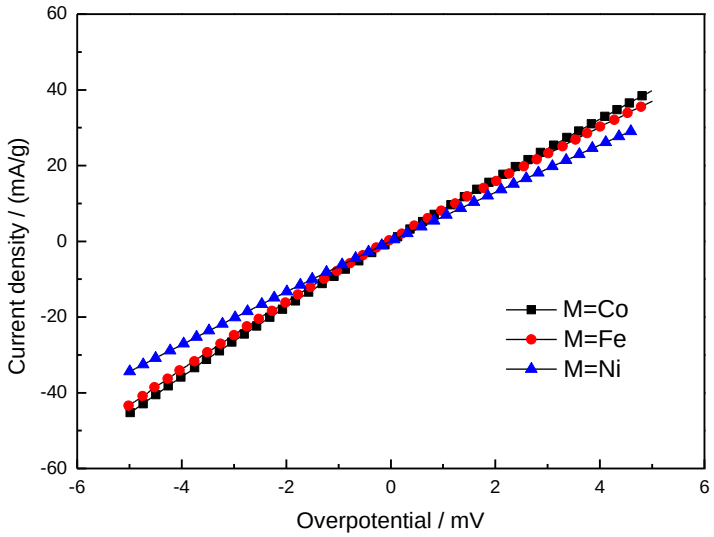

Figure 6. The linear polarization curves of $La_4MgNi_{17.5}M_{1.5}$ (M=Co, Fe, Mn) alloy electrodes

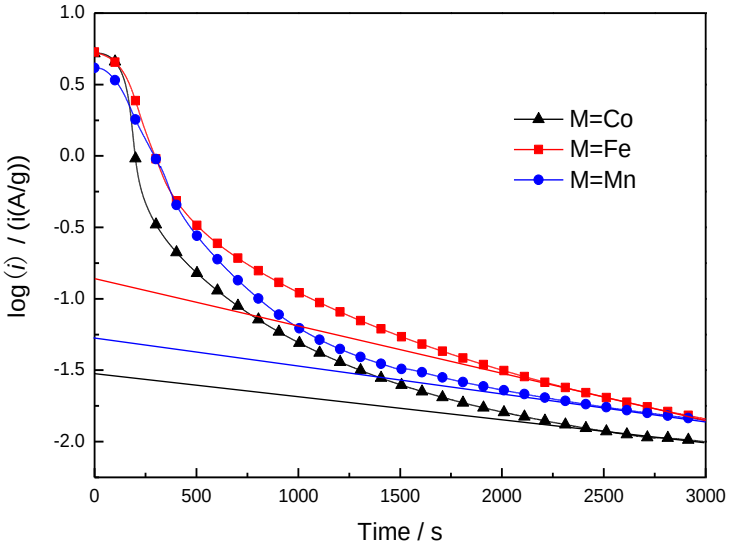

Figure 7. The Log(i)-Time responses curves of $La_4MgNi_{17.5}M_{1.5}$ (M=Co, Fe, Mn) alloy electrodes

It can be found that a moderate addition of Co can increase the exchange current density (I_0) of electrodes (240.32mA/g) and a suitable addition of Fe is beneficial for the diffusion of hydrogen atom

(*D*) in the bulk of the electrodes ($1.581\times10^{-10}cm^2s^{-1}$), which is consistent with the result studied by Gao et al[34]and Fan et al[28], respectively. Table 3 shows that the *D* correspond better with the variation of HRD while the I_0 has no obvious correlation with the HRD, which means the HRD of alloy electrodes are mainly controlled by the hydrogen diffusion coefficient in the crystal lattice.

4. CONCLUSION

The $La_4MgNi_{17.5}M_{1.5}$ (M=Co, Fe, Mn) alloys consist of AB_5-type phase ($CaCu_5$ structure) and A_5B_{19}-type phase (Ce_5Co_{19}+Pr_5Co_{19} structure). The cell volume of all the phases decrease in the order:Co<Fe<Mn. All the alloy electrodes can be activated within 3 cycles and the Mn substitution alloy electrode possess the highest discharge capacity about 367.3mAh/g. The cycling life of alloy electrodes follow the order: Co>Mn>Fe, which due to more serious pulverization of Fe substitution alloy. The moderate substitution by Co can increase the exchange current density (I_0) of electrodes and the suitable addition of Fe is beneficial for the diffusion of hydrogen atom (*D*) in the crystal lattice. The HRD of $La_4MgNi_{17.5}M_{1.5}$ (M=Co, Fe, Mn) alloy electrodes are mainly by the hydrogen diffusion coefficient in the crystal lattice.

ACKNOWLEDGMENTS
This work was supported by National Natural Science Foundation of China (50901036), Graduate Science and Technology Innovation Project of Jiangsu Province (KYLX16_0502), and Priority Academic Program Development of Jiangsu Higher Education Institutions

References

1. W. H. Zhu, Y. Zhu, Z. Davis and J. Bruce, *Applied Energy*, 106 (2013) 307.
2. E. C. E. Ronnebro and E. H. Majzoub, *MRS Bull*, 38 (2013) 452.
3. J. Y. Kim and I. Moon, *Int. J. Hydrogen Energy*, 33 (2008)7326.
4. M. A. Fetcenko ,S. Venkatesan and S. R. Ovshinsky, *Batteries and Electrochemistry*, 92 (1992) 141.
5. Y. Q. Lei, New energy materials, Tianjin: Tianjin University Press, China.
6. Y. Chen, H. G. Pan, R. G. Xu, S. Q. Li, L. X. Chen, C. P. Chen, and Q. D. Wang. *J. Alloys. Compd*, 648 (1999) 293.
7. Z. Q. Lan, J. C. Li, B. Wei, R. R. Zhu and J. Guo, *J. Rare. Earth*, 34 (2016) 401.
8. S. Muhammad, Balogun, Z. M. Wang, H. G. Zhang, Q. R. Yao, J. Q. Deng and H. Y. Zhou, *J. Alloys. Compd*, 438 (2013) 579.
9. T. Yang, T. T. Zhai, Z. M. Yuan, W. G. Bu, S. Xu and Y. H. Zhang, *J. Alloys. Compd*, 29 (2014) 617.
10. T. Kohno, H. Yoshida, F. Kawashima, T. Inaba, I. Sakai, M. Yamamoto and M. Kanda, *J. Alloys Compd*, 5 (2000) 311.
11. L. Z. Ouyang, Z. J. Cao, L. L. Li, H. Wang, J. W. Liu, D. Min, Y. W. Chen, F. M. Xiao, R. H. Tang and M. Zhu, *Int. J. Hydrogen Energy*, 39 (2014) 12765.
12. T. Yamamoto, H. Inui and M. Yamaguchi, *Acta. Metall*,5221 (1997) 5213.
13. X. B. Guo, Y. C. Luo, Z. J. Gao, G. Q. Zhang and L. Kang, *Journal of Functional Materials*, 18 (2012) 2450. (in Chinese)

14. Z. J. Cao, L. Z. Ouyang, L. L. Li, Y. S. Lu, H. Wang, W. Liu, D. Min, Y. W. Chen, F. M. Xiao, T. Sun, R. H. Tang and M. Zhu, *Int. J. Hydrogen Energy,* 451 (2015) 40.
15. Z. J. Cao, L. Z. Ouyang, H. Wang, J. W. Liu, D. L. Sun, Q. A. Zhang and M. Zhu, *J. Alloys. Compd,* 14 (2005) 608.
16. F. Li , K. Young ,T. Ouchi and M. A. Fetcenko, *J. Alloys. Compd*, 471 (2009) 371.
17. F. L. Zhang, Y. C. Luo, J. P. Chen, R. X. Yan, L. Kang and J. H. Chen, *J. Power Sources,* 150 (2005) 247.
18. C. L. Zhong, D. L. Chao, D. Zhu, Y. G. Chen, C. L. Wu and C. H. Xu, *Rare Metal Materials and Engineering*, 43 (2014) 519.
19. H. Miao, H. G. Pan, S. C. Zhang, N. Chen, R. Li and M. G. Gao, *Int. J. Hydrogen Energy*, 32 (2007) 3387.
20. B. Y. Qi, X. L. Han and R. Zhu, *Chinese Rare Earths*, 29 (2008) 53. (in Chinese)
21. Y. H. Zhang, C. Zhao, T. Yang, H. W. Shang, C. Xu and D. L. Zhao, *J. Alloys. Comp,* 131 (2013) 555
22. Y. H. Zhang, B. W. Li, H. P. Ren , Z. W. Wu , X. P. Dong and X. L. Wang, *Rare Metal Materials and Engineering,* 38 (2009) 941.
23. L. X. Chen, *Rare Metal Materials and Engineering*, 28 (1999) 302. (in Chinese)
24. S.Y.Ma.University Chemistry.8 (1993) 19 (in Chinese)
25. H. Shi, S. M. Han, Y. H. Jia, Y. Q. Liu, X. Zhao and B. Z. Liu, *Journal of Rare Earths,* 31 (2013) 79.
26. Y. H. Zhang, G. Q. Wang, X. P. Dong, S. H. Guo, J. Y. Ren and X. L. Wang, *J. Power Source*, 148 (2005) 105.
27. B. Z. Liu, A. M. Li, Y. P. Fan, M. J. Hu and B. Q. Zhang, *Transactions of Nonferrous Metals Society of China*, 22 (2012) 2730.
28. Y. P. Fan, X. Y. Peng, B. Z. Liu, B. Q. Zhang, Q. M. Peng and L. Q. Ji, *Int. J. Hydrogen Energy*, 39 (2014) 7042.
29. J. Gao, X. L. Yan, Z. Y. Zhao, Y. J. Chai and D. L. Hou, *J. Power Sources*, 257 (2012) 209.
30. T. Z. Huang, J. T. Han, Y. H. Zhang, J. M. Yu, G. X. Sun, H. Ren and X. X. Yuan, *J. Power Sources,* 196 (2011) 9585.
31. C. Iwakura, T. Oura, H. Inouse and M. Mastsuoka, *Electrochimica Acta*, 117 (1996) 41.
32. S. Tetsuo, M. Hiroshi, K. Nobuhiro, K. Akihiko, O. Keisuke, I. Hiroshi and I. Chiaki, *Journal of the Less Common Metals,* 159 (1990) 127.
33. F. S. Wei, Y. Q. Lei, L. X. Chen, D. Ying, H. W. Ge and G. L. Lv, *Transactions of Nonferrous Metals Society of China*, 16 (2006) 527.
34. Z. J. Gao,Y. Q. Luo, Z. Lin, R. F. Li, J. Y. Wang and L. Kang, *Journal of Rare Earths*, 28 (2010) 425.